

HS 0139+0559, HS 0229+8016, HS 0506+7725 and HS 0642+5049: Four new long-period cataclysmic variables*

A. Aungwerojwit¹, B.T. Gänsicke¹, P. Rodríguez-Gil^{1,2}, H.-J. Hagen³, E.T. Harlaftis⁴, C. Papadimitriou^{5,6},
H. Lehto^{7,8}, S. Araujo-Betancor⁹, U. Heber¹⁰, R.E. Fried¹¹, D. Engels³, and S. Katajainen⁸

¹ Department of Physics, University of Warwick, Coventry CV4 7AL, UK

² Instituto de Astrofísica de Canarias, 38200 La Laguna, Tenerife, Spain

³ Hamburger Sternwarte, Universität Hamburg, Gojenbergsweg 112, 21029 Hamburg, Germany

⁴ Institute of Space Applications and Remote Sensing, National Observatory of Athens, P.O. Box 20048, Athens 11810, Greece

⁵ Institute Astronomy and Astrophysics, National Observatory of Athens, P.O. Box 20048, Athens 11810, Greece

⁶ Department of Astrophysics, Astronomy and Mechanics, University of Athens, 157 84 Zografos, Athens, Greece

⁷ Department of Physics, FIN-20014 University of Turku, Finland

⁸ Tuorla Observatory, University of Turku, FIN-21500 Piikkiö, Finland

⁹ Space Telescope Science Institute, 3700 San Martin Drive, Baltimore, MD21218, USA

¹⁰ Astronomisches Institut der Universität Erlangen, Germany

¹¹ Braeside Observatory, PO Box906, Flagstaff, AZ 86002, USA

Received _____ ; accepted _____

Abstract. We present time-resolved optical spectroscopy and photometry of four relatively bright ($V \sim 14.0-15.5$) long-period cataclysmic variables (CVs) discovered in the Hamburg Quasar Survey: HS 0139+0559, HS 0229+8016, HS 0506+7725 and HS 0642+5049. Their respective orbital periods, 243.69 ± 0.49 min, 232.550 ± 0.049 min, 212.7 ± 0.2 min and 225.90 ± 0.23 min are determined from radial velocity and photometric variability studies. HS 0506+7725 is characterised by strong Balmer and He emission lines, short-period ($\sim 10-20$ min) flickering and weak X-ray emission in the ROSAT All Sky Survey. The detection of a deep low state ($B \simeq 18.5$) identifies HS 0506+7725 as a member of the VY Scl stars. HS 0139+0559, HS 0229+8016 and HS 0642+5049 display thick-disc like spectra and no or only weak flickering activity. HS 0139+0559 and HS 0229+8016 exhibit clean quasi-sinusoidal radial velocity variations of their emission lines but no or very little orbital photometric variability. In contrast, we detect no radial velocity variation in HS 0642+5049 but a noticeable orbital brightness variation. We identify all three systems either as UX UMa-type novalike variables or as Z Cam-type dwarf novae. Our identification of these four new systems underlines that the currently known sample of CVs is rather incomplete even for bright objects. The four new systems add to the clustering of orbital periods in the 3–4 h range found in the sample of HQS selected CVs, and we discuss the large incidence of magnetic CVs and VY Scl/SW Sex stars found in this period range among the known population of CVs.

Key words. stars: binaries: close – stars: individual: HS 0139+0559, HS 0229+8016, HS 0506+7725, HS 0642+5049 – stars: novae, cataclysmic variables

Send offprint requests to: A. Aungwerojwit,
e-mail: A.Aungwerojwit@warwick.ac.uk

* Based on observations obtained at the German-Spanish Astronomical Center, Calar Alto, operated by the Max-Planck-Institut für Astronomie, Heidelberg, jointly with the Spanish National Commission for Astronomy, on observations made at the 1.2m telescope, located at Kryoneri Korinthias, and owned by the National Observatory of Athens, Greece, on observations made with the OGS telescope, operated on the island of Tenerife by the European Space Agency, in the Spanish Observatorio del Teide of the IAC.

1. Introduction

Standard models for the population of cataclysmic variables (CVs) predict that the vast majority of all CVs should have short orbital periods, $P_{\text{orb}} < 2$ h (e.g. Kolb 1993; Howell et al. 1997), and a space density of $2 \times 10^{-5} - 2 \times 10^{-4} \text{ pc}^{-3}$ (Ritter & Burkert 1986; de Kool 1992; Politano 1996). These predictions are in contrast with the properties of the observed population of galactic CVs, with an estimated space density of $\sim 6 \times 10^{-6} \text{ pc}^{-3}$ (Ringwald 1996; Araujo-Betancor et al. 2005b) and an

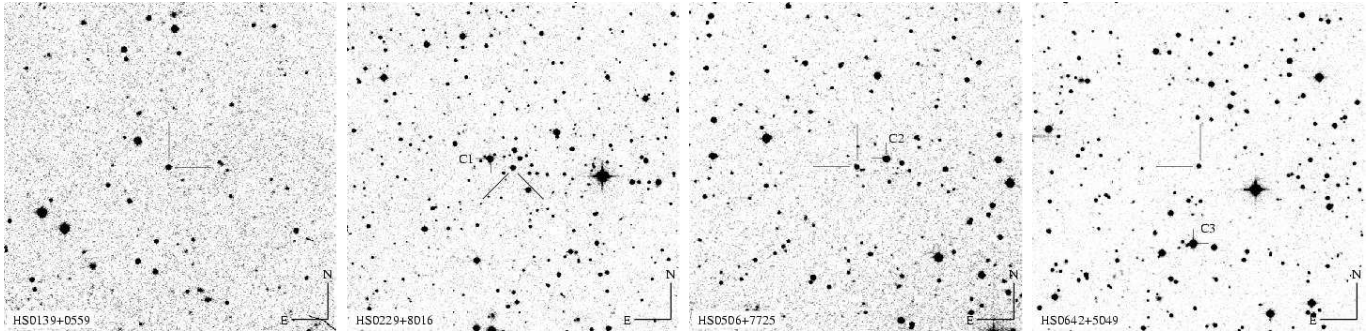


Fig. 1. $10' \times 10'$ finding charts for HS 0139+0559, HS 0229+8016, HS 0506+7725 and HS 0642+5049 obtained from the Digitized Sky Survey. The J2000 coordinates of the CVs are $(\alpha = 01^{\text{h}}41^{\text{m}}40.0^{\text{s}}, \delta = +06^{\circ}14'36.8'')$, $(\alpha = 02^{\text{h}}35^{\text{m}}58.3^{\text{s}}, \delta = +80^{\circ}29'44.0'')$, $(\alpha = 05^{\text{h}}13^{\text{m}}36.4^{\text{s}}, \delta = +77^{\circ}28'42.1'')$ and $(\alpha = 06^{\text{h}}46^{\text{m}}19.60^{\text{s}}, \delta = +50^{\circ}45'48.0'')$, respectively.

apparent lack of short-period systems. Possible reasons for these discrepancies are uncertainties in the theory of CV evolution (e.g. King 1988; Schenker & King 2002; Andronov et al. 2003; Barker & Kolb 2003; Taam et al. 2003), but also observational selection effects in the known CV population (e.g. Downes 1986; Ringwald 1996; Gänsicke 2005).

2. CVs in the Hamburg Quasar Survey

About 75% of all known CVs have been discovered either because of their variability or because of their X-ray emission, with a strong dominance of dwarf novae and classical nova in the first group and magnetic CVs in the second group (Gänsicke 2005). It is therefore clear that CVs which are characterised by infrequent outbursts and/or low-amplitude variability, as well as lacking strong X-ray emission, will be underrepresented in the currently known CV population. Hypothetically, such objects could make up for the large number of predicted short-period CVs with low mass transfer rates.

The primary purpose for our project identifying new CVs in Hamburg Quasar Survey (HQS) is to establish a large homogeneously selected sample of systems that overcomes previous observational biases, and that can subsequently be used to test our understanding of CV evolution (Gänsicke et al. 2002b). The HQS, an objective-prism survey, has been carried out with the 0.8 m Schmidt telescope at Calar Alto Observatory to search for bright quasars in the northern sky at high galactic latitudes, $\delta > 0^{\circ}$ and $|b| > 20^{\circ}$, covering $\approx 13\,600 \text{ deg}^2$, with a dynamic range of $13 \lesssim B \lesssim 18.5$ (Hagen et al. 1995). The photographic plates covered a spectral range of $\sim 3400 - 5400 \text{ \AA}$ with a resolution of $\sim 45 \text{ \AA}$ at $H\beta$.

Our CV candidate selection made use of a property that has never been systematically exploited before: the *spectroscopic* hallmark of CVs, i.e. the presence of noticeable emission lines in most CVs. The CV candidate selection was carried out by visually inspecting 48708 HQS prism spectra for the presence of Balmer emission lines. In order to test the efficiency of this method, we applied the same procedure to the subset of 84 previously known CVs

(Downes et al. 2001, as of July 2001) that are contained in the HQS spectral data base. We positively recovered $\simeq 90\%$ of the known short-period ($P_{\text{orb}} < 2 \text{ h}$) CVs, including prominent dwarf novae such as SW UMa or T Leo (the latter one has a rather long outburst cycle of $\sim 420 \text{ d}$), as well as magnetic CVs such as AN UMa or ST LMi. The fraction of recovered systems drops to $\simeq 40\%$ for long-period systems, with the largest fraction of missed identifications being novalike variables with weak or no Balmer emission lines. In total, 62% of the previously known CVs having an HQS prism spectrum were positively identified by our selection method. We concluded from this test that the HQS should be very efficient in finding CVs below the period gap as long as they have similar spectroscopic properties to the previously known systems, i.e. Balmer emission lines with equivalent widths $> 10 \text{ \AA}$ in $H\beta$. The decrease in detection efficiency for long-period systems has been compensated to some extent by follow-up programs investigating hot stars in the HQS, delivering a number of new CVs with weak emission lines (Heber et al. 1991).

In total, 53 new CVs were identified within this project, and a substantial observational effort has been invested to determine the properties of these systems. To date, 42 HQS CVs have had their orbital period measured. Despite its good sensitivity for short-period CVs, only a small number of new short-period CVs has been found, and those that have been found fully confirm the expected properties: low-amplitude variability and/or long outburst recurrence times, e.g. KV Dra (HS 1449+6415, Nogami et al. 2000); HS 2331+3905 (Araujo-Betancor et al. 2005a), DW Cnc (HS 0756+1624, Rodríguez-Gil et al. 2004a), or HS 2219+1824 (Rodríguez-Gil et al. 2005a). The majority of the newly identified systems have orbital periods above the 2 – 3 h period gap, including rarely outbursting dwarf novae such as GY Cnc (HS 0907+1902, Gänsicke et al. 2000) or RX J0944.5+0357 (HS0941+0411, Mennickent et al. 2002); magnetic CVs with relatively weak X-ray emission, such as 1RXS J062518.2+733433 (HS0618+7336, Araujo-Betancor et al. 2003), RX J1554.2+2721 (HS 1552+2730, Thorstensen & Fenton

2002; Gänsicke et al. 2004b) and HS 0943+1404 (Rodríguez-Gil et al. 2005b); and half a dozen new SW Sextantis stars (Gänsicke et al. 2002c; Szkody et al. 2001; Rodríguez-Gil et al. 2004b; Rodríguez-Gil 2005).

While a full discussion of the implications that our search for CVs in the HQS has for our understanding of the galactic CV population has to await the characterization of the full HQS CV sample, an important preliminary statement that will not substantially change is *there is no substantial population of nearby short-period CVs that resemble the known template systems*. Phrased differently, if the large population of short period CVs predicted by theory exists, the majority of these systems must look different from the known short-period systems, i.e. have weak emission lines and/or substantially redder continua. Interestingly, the Sloan Digital Sky Survey (SDSS) is discovering a number of CVs with a steep Balmer decrement and in which the white dwarf dominates the optical emission, a clear sign of low mass transfer rates (Szkody et al. 2005, and references therein). However, most of these systems are very faint, $g \simeq 19 - 20$, implying that they are distant ($d > 100$ pc) and not intrinsically numerous anywhere near the numbers predicted by theory.

An unexpected finding of our search for CVs in the HQS has been the identification of a large number of systems with orbital periods in the range 3 – 4 h. Here, we report the discovery of four additional CVs in that period range, HS 0139+0559, HS 0229+8016, HS 0506+7725 and HS 0642+5049. Despite being close in orbital period, these systems differ dramatically in their observed characteristic, and we discuss in detail the properties of the known CVs in the 3 – 4 h period range.

3. Observations and Data Reduction

3.1. Spectroscopy

An identification spectrum of HS 0139+0559 (see finding chart in Fig. 1) was obtained in October 1989 at the Calar Alto 3.5 m telescope using the Boller&Chivens spectrograph equipped with a 120Å/mm grating as part of a program to find blue stars (Heber et al. 1991). This spectrum (Fig. 2) is characterised by a blue continuum with strong absorption lines of the Balmer series as well as of He I $\lambda 4471$. The absorption profiles have a rectangular shape with a full width at zero intensity (FWZI) of $\sim 3500 \text{ km s}^{-1}$. The cores of H β and H γ broad absorptions show weak emission lines. No He II $\lambda 4686$ is observed. Overall, the spectrum resembles that of a high-mass transfer rate accretion disc seen at a moderately low inclination, e.g. a dwarf nova in outburst or a novalike variable.

HS 0229+8016 (Fig. 1) was first spectroscopically observed at the Calar Alto 2.2 m telescope on 1982 August 8, using the Boller & Chivens spectrograph. The spectrum (Fig. 3, top panel) shows a blue continuum with the Balmer jump in emission, superimposed by moderately strong Balmer emission lines. The higher Balmer line profiles show evidence for a P-Cygni like structure

with blue absorption wings increasing in strength for the higher members of the series. He I $\lambda 4471$ is observed in absorption, and an emission line near 4630 Å is detected, that we tentatively identify as the N/C Bowen blend emission. Rather unusual is, however, the fact that He II $\lambda 4686$ is not detected in emission along with the Bowen blend. HS 0229+8016 was observed again at the Calar Alto 2.2 m telescope on 1998 October 5 using the Calar Alto Faint Object Spectrograph (CAFOS), on this occasion looking nearly identical to HS 0139+8016 (Fig. 3, bottom panel). The spectral characteristics and the variability clearly identify HS 0229+8016 as a CV.

An identification spectrum of HS 0506+7725 (Fig. 1) was obtained on 1998 February 2 on the Calar Alto 2.2 m telescope using CAFOS with the B-400 grism. The spectrum (Fig. 4) displays a blue continuum with the Balmer and Paschen jumps in emission, plus emission lines of hydrogen and He I. The $\lambda\lambda 4630 - 4650$ N/C Bowen blend and the He II $\lambda 4686$ emission lines are also detected. The strength of these high-ionisation lines is typical of novalike variables, magnetic CVs or nova remnants.

HS 0642+5049 (Fig. 1) was spectroscopically identified as a CV on 1999 March 7 with CAFOS at the Calar Alto 2.2 m telescope. The spectrum of HS 0642+5049 (Fig. 5) contains a blue continuum with moderately strong H α emission. The H β and H γ emission is embedded in broad absorption troughs, and weak He I $\lambda 4471$ absorption is also detected. No He II $\lambda 4686$ and $\lambda\lambda 4630 - 4650$ N/C Bowen blend are detected.

In order to determine the orbital periods of HS 0139+0559, HS 0229+8016, HS 0506+7725 and HS 0642+5049 we obtained time-resolved spectroscopy at Calar Alto Observatory and Roche de los Muchachos Observatory throughout the period October 2002 to October 2004 (Table 1). At the Calar Alto 2.2 m telescope, we used the CAFOS spectrograph equipped with the G-100 grating and a $2k \times 2k$ pixel SITe CCD. This setup, in conjunction with a 1.2" slit, provided a spectral resolution of $\sim 4.1 \text{ \AA}$ (full width at half maximum, FWHM) covering the range 4240–8300 Å. We used the double-armed TWIN spectrograph at the Calar Alto 3.5 m telescope equipped with the T05 grating in the blue and the T06 grating in the red, providing a spectral resolution of $\sim 1.2 \text{ \AA}$ (FWHM) in the ranges $\lambda\lambda 3810 - 4940$ and $\lambda\lambda 6440 - 7510$. At the 2.5 m Isaac Newton Telescope (INT), we used the Intermediate Dispersion Spectrograph (IDS) equipped with the R632V grating and the $2k \times 4k$ pixel EEV10a detector. Using a slit width of 1.5" this setup provided a useful wavelength of $\sim 4400 - 6800 \text{ \AA}$ and a spectral resolution of $\sim 2.3 \text{ \AA}$. Arc calibration spectra were interleaved with the target observations every ~ 40 min.

In total, we obtained 55 spectra of HS 0139+0559, 74 spectra of HS 0229+8016, 86 spectra of HS 0506+7725 and 87 spectra of HS 0642+5049 (Table 1). The reduction of the follow-up spectroscopy consisting of bias and flat-field corrections and optimal extraction (Horne 1986) was car-

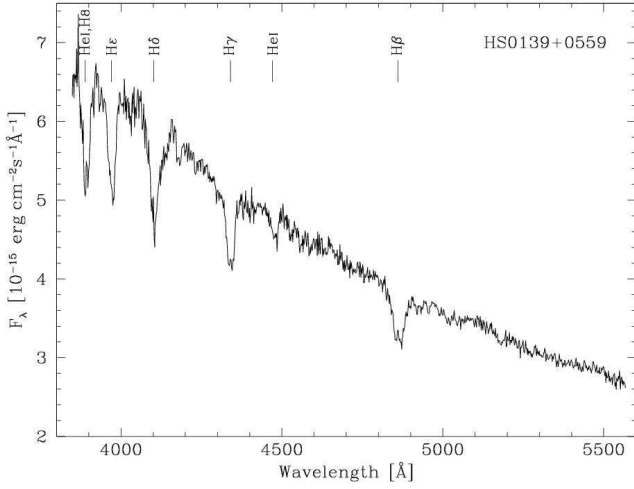


Fig. 2. Identification spectrum of HS 0139+0559 obtained at the Calar Alto 3.5 m telescope on 1989 January 22.

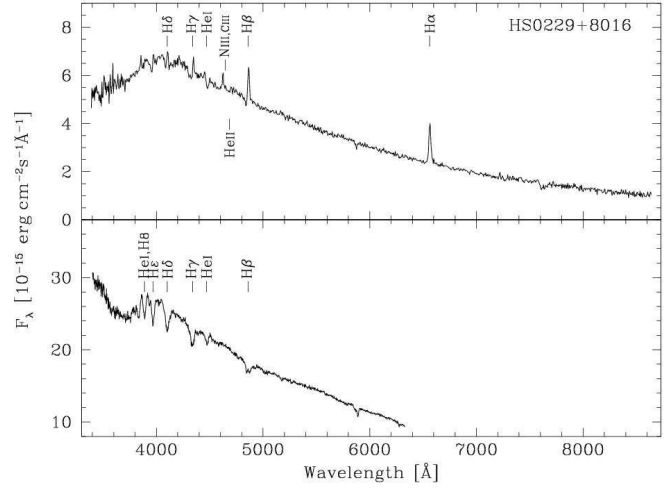


Fig. 3. Identification spectra of HS 0229+8016 obtained at the Calar Alto 2.2 m telescope on 1992 August 8 (top panel) and 1998 February 2 (bottom panel).

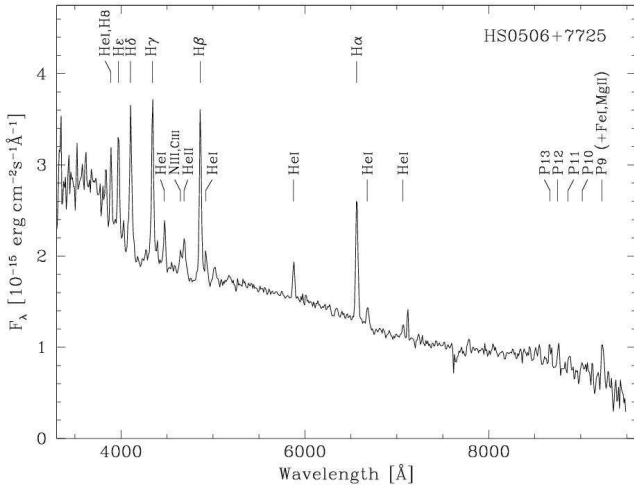


Fig. 4. Identification spectrum of HS 0506+7725 obtained at the Calar Alto 2.2 m telescope on 1998 February 2.

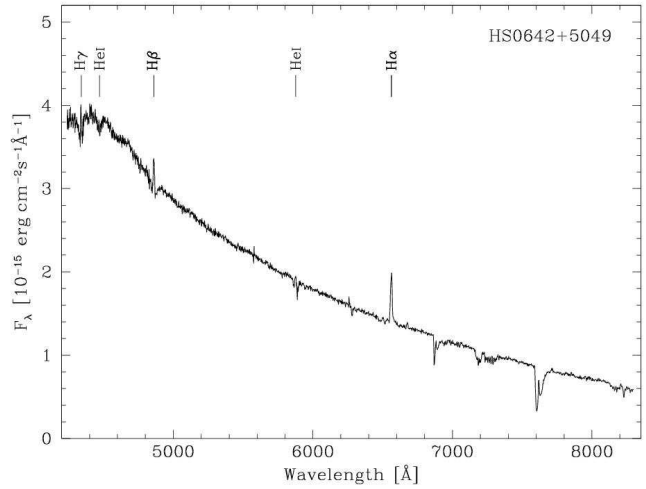


Fig. 5. Average of the 17 CAFOS G-100 spectra of HS 0642+5049 obtained at the Calar Alto 2.2 m telescope on 2004 October 24.

ried out in IRAF.¹ The wavelength calibration of the extracted spectra was performed in MOLLY. The dispersion relation was obtained by fitting a low-order polynomial to the arc lines, with the RMS being less than one tenth of the dispersion in all cases. The flexure of the telescope was accounted for by interpolating between the two arc exposures bracketing the target spectra.

The time-resolved spectra of HS 0139+0559, HS 0229+8016 are similar to the identification spectra shown in Fig. 2 and Fig. 3 (bottom panel), with H β and H γ in absorption for most of the time, and occasionally showing signs of emission cores. However, the G-100 spectra cover H α as well, which is observed in emission throughout, with low equivalent widths in the range 3–6 Å. The time-resolved spectra of HS 0506+7725

are very similar to the identification spectrum shown in Fig. 4, with difference of having no He II λ 4686 emission. The H α emission line has an average equivalent width of ~ 15 Å. The time-resolved spectra of HS 0642+5049 show H α in emission with an average equivalent width of ~ 5 Å, and weak H β and H γ emission embedded in broad absorption lines (Fig. 5).

3.2. Photometry

The spectroscopy of the four new cataclysmic variables was supplemented by differential CCD photometry obtained at six different telescopes (Table 1). Brief descriptions of the used instrumentation and the data reduction techniques are given below.

¹ IRAF is distributed by the National Optical Astronomy Observatories.

Table 1. Log of the observations.

Date	UT Time	Filter/ Grating	Exp. (s)	Frames	Mean mag.	Date	UT Time	Filter/ Grating	Exp. (s)	Frames	Mean mag.
HS 0139+0559						Spectroscopy: Hamburg-Schmidt telescope at Calar Alto					
Spectroscopy: Calar Alto 3.5 m & B&C						1987 Oct 29	-	Prism	3600	1	$\simeq 15.1$
1989 Jan 22	19:21	120Å/mm	900	1	-	1994 Jan 12	-	Prism	3600	1	$\simeq 15.3$
Spectroscopy: Calar Alto 3.5 m & TWIN						1995 Oct 23	-	Prism	3600	1	$\simeq 18.3$
2002 Oct 28	23:53-00:03	T08/T01	300	1	-	Photometry: Kryoneri Observatory					
2002 Oct 29	22:36-03:21	T05/T06	600	16	-	2002 Oct 08	22:46-01:25	<i>R</i>	10	599	$\simeq 15.2$
Spectroscopy: Calar Alto 2.2 m & CAFOS						Photometry: Tuorla Observatory					
2003 Dec 24	18:25-00:10	G-100	600	27	$\simeq 15.4$	2003 Jan 04	16:13-20:16	Clear	120	32	$\simeq 15.7$
2003 Dec 26	18:34-20:48	G-100	600	12	$\simeq 15.1$	2003 Jan 06	15:47-20:46	Clear	60	213	$\simeq 15.8$
Spectroscopy: Hamburg-Schmidt telescope at Calar Alto						2003 Jan 16	20:18-22:40	Clear	60	115	$\simeq 15.9$
1981 Nov 01	-	Prism	3600	1	$\simeq 14.9$	Photometry: OGS					
1981 Nov 02	-	Prism	3600	1	$\simeq 14.9$	2003 Nov 15	03:21-06:37	Clear	5	1110	$\simeq 14.6$
Photometry: Braeside Observatory						Photometry: Calar Alto 2.2 m & CAFOS					
1999 Dec 30	02:15-07:04	<i>R</i>	70	293	-	2003 Jan 01	01:01-03:24	<i>V</i>	30	85	$\simeq 15.1$
2000 Jan 04	02:31-06:04	<i>B</i>	50	136	-	2003 Dec 16	00:05-05:11	Clear	15-30	346	$\simeq 14.8$
HS 0229+8016						2003 Dec 25	19:15-02:29	Clear	15-30	296	$\simeq 14.9$
Spectroscopy: Calar Alto 2.2 m & B&C						2003 Dec 27	04:03-06:16	Clear	20	149	$\simeq 14.9$
1992 Aug 08	03:16		900	1	$\simeq 15.0$	2003 Dec 27	20:33-23:55	Clear	20	288	$\simeq 14.8$
Spectroscopy: Calar Alto 2.2 m & CAFOS						HS 0642+5049					
1998 Oct 05	01:37	B-200	1800	1	$\simeq 13.7$	Spectroscopy: Calar Alto 2.2 m & CAFOS					
2003 Dec 14	19:18-00:55	G-100	600	24	$\simeq 14.2$	1999 Mar 07	19:11	B-400	300	1	-
2003 Dec 16	20:21-03:08	G-100	600	27	-	2003 Apr 27	20:03-21:53	G-100	600	9	$\simeq 15.6$
2003 Dec 23	18:49-21:01	G-100	600	12	$\simeq 14.5$	2003 May 10	20:20-21:21	G-100	600	6	-
2003 Dec 26	21:34-22:53	G-100	600	7	$\simeq 14.1$	2003 May 11	20:17-21:20	G-100	600	6	-
2003 Dec 27	18:46-19:22	G-100	600	4	$\simeq 13.7$	2003 Dec 25	00:56-05:35	G-100	600	24	$\simeq 15.5$
Spectroscopy: Hamburg-Schmidt telescope at Calar Alto						2003 Dec 27	02:50-03:01	G-100	600	2	$\simeq 15.3$
1986 Nov 05	-	Prism	3600	1	$\simeq 14.4$	2004 Oct 24	02:12-05:26	G-100	600	17	$\simeq 15.3$
1986 Nov 06	-	Prism	3600	1	$\simeq 14.2$	2004 Oct 26	04:25-05:31	G-100	600	7	$\simeq 15.4$
1994 Nov 12	-	Prism	3600	1	$\simeq 14.6$	Spectroscopy: INT 2.5 m & IDS					
Photometry: Kryoneri Observatory						2003 Apr 25	21:21-22:14	R632V	600	6	-
2002 Sep 20	01:30-03:28	<i>R</i>	5	840	$\simeq 14.2$	2003 Apr 26	21:17-21:49	R632V	600-900	4	-
2002 Sep 20	22:37-03:27	<i>R</i>	5	1680	$\simeq 14.3$	2003 Apr 28	21:15-22:08	R632V	600	6	-
Photometry: Tuorla Observatory						Spectroscopy: Hamburg-Schmidt telescope at Calar Alto					
2003 Jan 10	15:41-23:45	Clear	30	695	$\simeq 14.3$	1991 Nov 10	-	Prism	3600	1	$\simeq 15.8$
HS 0506+7725						1993 Oct 24	-	Prism	3600	1	$\simeq 16.0$
Spectroscopy: Calar Alto 3.5 m & TWIN						Photometry: Tuorla Observatory					
2002 Dec 03	03:22-05:09	T05/T06	600	10	-	2003 Dec 30	19:58-21:06	Clear	120	46	$\simeq 15.4$
Spectroscopy: Calar Alto 2.2 m & CAFOS						2004 Jan 01	18:37-23:27	Clear	60	250	$\simeq 15.5$
1998 Feb 02	19:43	B-400	180	1	-	Photometry: Calar Alto 2.2 m & CAFOS					
2002 Dec 09	00:19-00:30	G-100	600	2	$\simeq 15.4$	2003 Dec 26	04:20-06:14	Clear	20-30	149	$\simeq 15.6$
2003 Dec 13	23:25-03:53	G-100	600	23	$\simeq 14.7$	2004 Oct 22	04:01-05:25	Clear	15	59	$\simeq 15.7$
2003 Dec 15	01:34-06:13	G-100	600	23	$\simeq 14.9$	2004 Oct 25	01:42-05:51	Clear	10-15	463	$\simeq 15.5$
2003 Dec 17	03:40-05:57	G-100	600	12	-	Photometry: IAC80					
2003 Dec 23	22:19-00:31	G-100	600	12	$\simeq 14.9$	2004 Dec 02	04:01-05:00	Clear	10	150	$\simeq 15.4$
2003 Dec 26	02:52-03:28	G-100	600	4	$\simeq 14.9$	2004 Dec 07	05:10-06:11	Clear	15	139	$\simeq 15.3$
						2004 Dec 08	01:00-04:41	Clear	10	528	$\simeq 15.3$
						2004 Dec 09	00:13-05:14	Clear	10	738	$\simeq 15.3$

Braeside Observatory. Differential *B* and *R* photometry of HS 0139+0559 was obtained in December 1999/January 2000 at Braeside Observatory using the 0.41 m reflector together with a SITE 512 × 512 pixel CCD camera. The raw images were bias-subtracted, dark current-subtracted and flat-fielded in a standard manner.

Kryoneri Observatory. We obtained differential *R*-band photometry of HS 0229+8016 (2002 September 19 & 20) and HS 0506+7725 (2002 October 8) at Kryoneri Observatory using the 1.2 m telescope equipped with a Photometrics SI-502 516 × 516 pixel CCD camera. The data were reduced using the pipeline described in Gänsicke et al. (2004a), which pre-processes the raw images in MIDAS and extracts aperture photometry using the

SExtractor (Bertin & Arnouts 1996). The instrumental magnitudes of HS 0229+8016 were converted into apparent magnitudes using the comparison star labelled 'C1' in Fig. 1 (USNO-A2.0 1650-00512682, $R = 12.6$). We found a mean magnitude of $R \simeq 14.3$ during both nights. The apparent magnitudes of HS 0506+7725 were computed using the comparison star 'C2' (USNO-A2.0 1650-00942250, $R = 13.1$), and an average magnitude of $R \simeq 15.2$ was found.

Tuorla Observatory. We used the 0.7 m Schmidt-Vaisala telescope at Tuorla Observatory, equipped with a SBIG ST-8 CCD camera to obtain filterless photometry of HS 0229+8016 (2003 January 10), HS 0506+7725 (2003 January 4, 6 & 16) and HS 0642+5049 (2003 December 30 & 2004 January 1). The reduction of the observations was carried out in the same way as described for the Kryoneri data. Using the same comparison stars as above, we found the mean magnitudes of HS 0229+8016 and HS 0506+7725 to be $\simeq 14.3$ and $\simeq 15.8$, respectively. The apparent magnitudes of HS 0642+5049 were extracted using the comparison star 'C3' in Fig. 1 (USNO-A2.0 1350-06806656, $R = 12.4$), and gave a mean magnitude of $\simeq 15.5$.

Observatorio del Teide. At the Observatorio del Teide on Tenerife we used the 1 m Optical Ground Station (OGS) and the 0.82 m IAC80 telescopes to obtain CCD photometry of HS 0506+7725 and HS 0642+5049. The telescopes were equipped with Thomson 1k \times 1k pixel CCD cameras. On 2003 November 15, the OGS was used to obtain differential photometry of HS 0506+7725 in white light. The data were taken using 2×2 binning and windowing to improve the time resolution. The images were bias and flat-field corrected and aligned within IRAF. Instrumental magnitudes of the CV and the comparison star 'C2' were then extracted using the point spread function (PSF) photometry tasks package within IRAF. We found the mean magnitude of HS 0506+7725 during that night to be $\simeq 14.6$. On 2004 December 1, 6, 7 & 8, we used the IAC80 telescope to obtain filterless photometry of HS 0642+5049. In order to achieve a high time resolution, windowing and binning 2×2 were applied. The data were reduced using MIDAS in the same manner as described for the Kryoneri run. The apparent magnitudes were extracted using the comparison star 'C3', resulting in a mean magnitude of $\simeq 15.3$.

Calar Alto Observatory. During January 2003 and October 2004, we used CAFOS with the SITe 2k \times 2k pixel CCD camera on the 2.2 m telescope to obtain filterless differential photometry of HS 0506+7725 and HS 0642+5049 when the atmospheric conditions were too poor for spectroscopy. Only a small part of the CCD was read out in order to improve the time resolution. The data were reduced in an analogous fashion as described for the Kryoneri observations above. The mean magnitudes of HS 0506+7725

and HS 0642+5049 were found to be $\simeq 14.9$ and $\simeq 15.6$ respectively.

Light curve morphology. The light curves of HS 0139+0559 (Fig. 6) and HS 0229+8016 (Fig. 7) display very little variability on nightly time scales, with amplitudes $\lesssim 0.02$ mag and ~ 0.05 mag, respectively. In the case of HS 0229+8016, a low-amplitude modulation with a period of ~ 4 h is consistently detected during the two longest observations. HS 0506+7725 exhibits short-period variability with an amplitude of $\sim 0.2 - 0.4$ mag which appear to be quasi-periodic oscillations on time scales of $\sim 10 - 20$ min (Fig. 8). No clearly repeating variation is detected on time scales of several hours (i.e. a putative orbital modulation). The light curves of HS 0642+5049 from the IAC80 (Fig. 9) show a modulation with a period of ~ 3.5 hr which we interpret as the orbital period of the system. No substantial flickering activity is detected.

The USNO-A2.0 catalogue lists HS 0139+0559 with $B = R = 14.4$ and we found $V \simeq 15.4$ and $B \simeq 14.9$ in our observations. HS 0229+8016 has $B = 13.9$ and $R = 13.8$ in the USNO-A2.0 catalogue, and has been found during our observations mostly near $B \simeq V \simeq 14.0 - 14.6$, except on one occasion (August 1992) when it was as faint as $V \simeq 15.0$ mag. HS 0506+7725 is listed with $B = 15.3$ and $R = 15.6$ in the USNO-A2.0 catalogue, and our data provides evidence for long-term variability of the mean magnitude by ~ 1 mag, but dropping on one occasion (October 1995) into a deep low state at $B \simeq 18.3$. HS 0642+5049 is found in the USNO-A2.0 catalogue with $B = 16.6$ and $R = 16.9$ and we found $V \simeq 15.3 - 15.5$ mag without significant long-term variability of the system.

4. Analysis

4.1. HS 0139+0559

In order to determine the orbital period of HS 0139+0559 we have measured the radial velocity variations of H α by convolving the observed line profiles with a single Gaussian of FWHM=600 km s $^{-1}$. The spectra were continuum-normalised prior to this analysis. A Scargle (1982) period analysis of the radial velocity measurements was performed using the MIDAS/TSA context. The resulting periodogram (Fig. 10) shows a strong signal at 5.909 ± 0.012 d $^{-1}$ (where the error is determined from fitting a sine wave to the radial velocity variation, see Table 2 for the full fit parameter), surrounded by one-day aliases. In order to test the significance of the detected signal, we have created a set of fake radial velocities by evaluating a sine function with a frequency of 5.909 d $^{-1}$ at the exact times of the observed spectroscopic data. The amplitude of the sine wave was adjusted to reflect the observed radial velocity amplitude, and the fake radial velocity measurements were randomly offset from the computed sine wave using the observed errors. The periodogram of the fake data reproduces the alias structure of the periodogram computed from the observations very well.

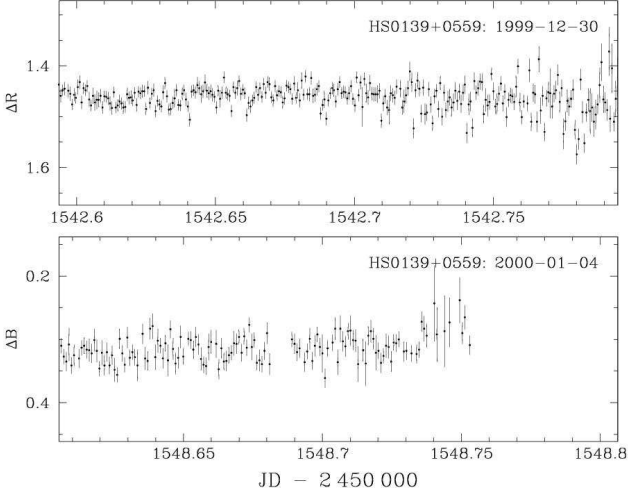


Fig. 6. Differential CCD *R*-band (top panel) and *B*-band (bottom panel) photometry of HS 0139+0559 obtained at the Braeside observatory.

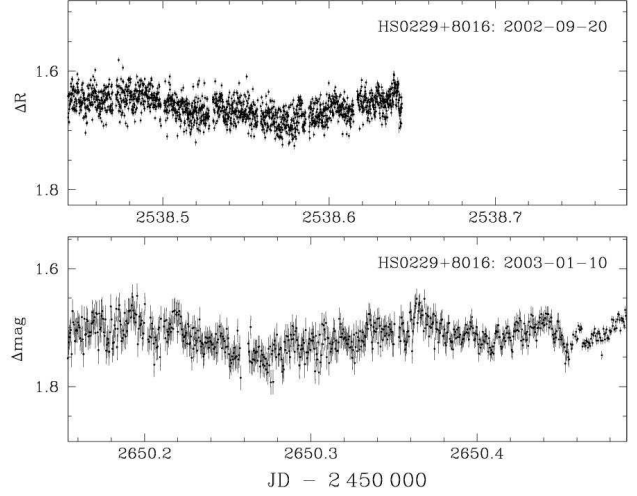


Fig. 7. Sample light curves of HS 0229+8016. Top panel: *R*-band data obtained at the Kryoneri observatory. Bottom panel: filterless data obtained at the Tuorla observatory.

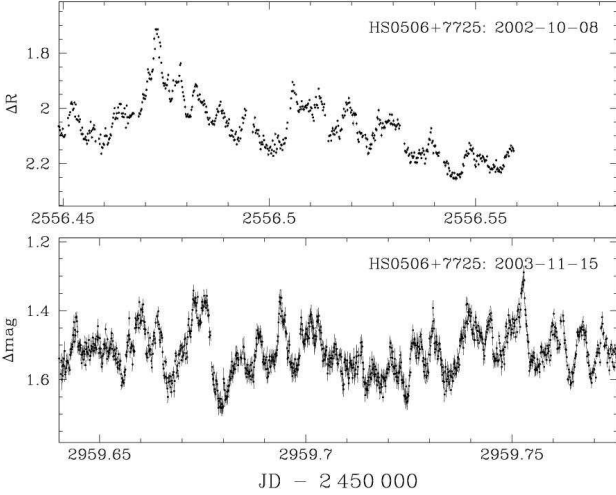


Fig. 8. Sample light curves of HS 0506+7725. Top panel: *R*-band data obtained at the Kryoneri observatory. Bottom panel: filterless data obtained at the OGS telescope.

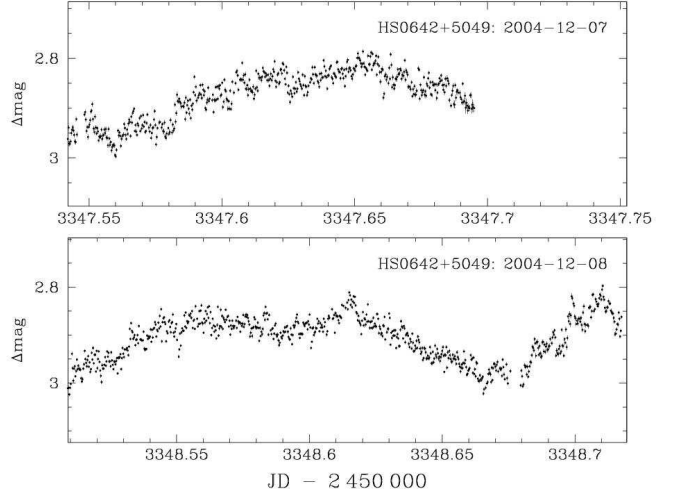


Fig. 9. Sample filterless light curves of HS 0642+5049 obtained at the IAC80 telescope.

We conclude that the orbital period of HS 0139+0559 is $P_{\text{orb}} = 243.69 \pm 0.49$ min. Folding the radial velocity measurements over that period results in a quasi-sinusoidal radial velocity curve with an amplitude of 84.4 ± 4.8 km s⁻¹ (Fig. 14, top panel).

For completeness, we have also used the Braeside *B* and *R* band photometry for a period analysis. As suggested by the flat light curve (Fig. 6) no significant signal is detected in the Scargle periodogram.

4.2. HS 0229+8016

An analogous radial velocity analysis as described in the previous section was carried out for HS 0229+8016. Inspection of the Scargle periodogram (Fig. 11) shows a

somewhat more complex alias structure as a result of the inhomogeneous spacing of the spectroscopic observations. The strongest signal is found at 6.1922 ± 0.0013 d⁻¹ (where the error is again computed from a sine fit to the radial velocity data, Table 2) and a fake data set computed using this frequency reproduces well the overall alias structure. We conclude that the most likely value for the orbital period of HS 0229+0559 is $P_{\text{orb}} = 232.550 \pm 0.049$ min. The phase-folded radial velocity curve shows a quasi-sinusoidal modulation with an amplitude of 179.0 ± 5.2 km s⁻¹ (Table 2).

Scargle periodograms computed from the two longest photometry runs on HS 0229+0559 are dominated by a broad signal near 5.2 d⁻¹ (Kryoneri data) and 6.2 d⁻¹ (Tuorla), which are consistent with the spectroscopic pe-

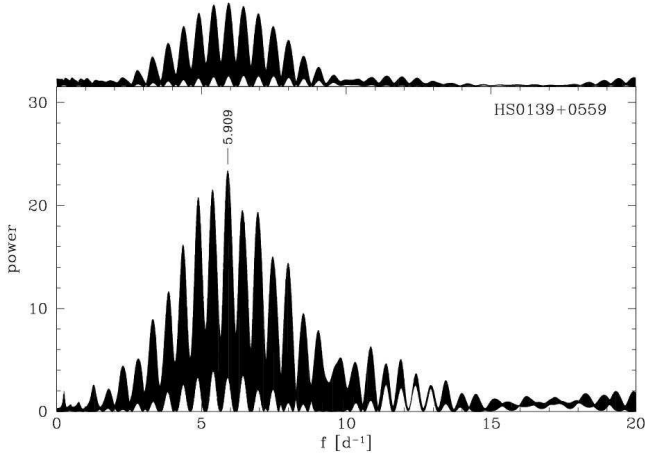


Fig. 10. The Scargle periodogram of the radial velocities of HS 0139+0559 measured from the H α emission line. The periodogram from a set of fake radial velocities is shown in the top panel.

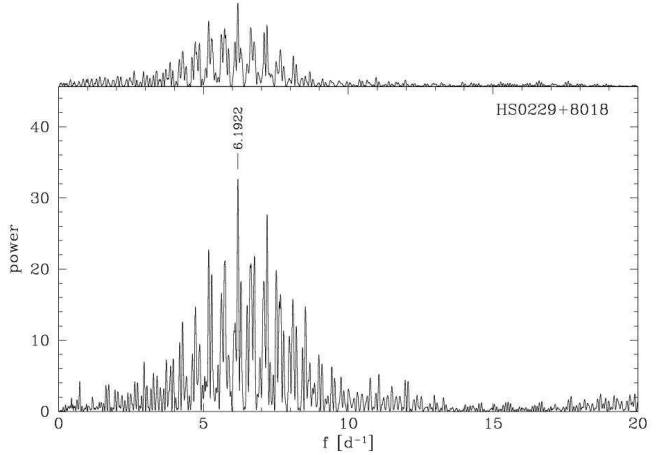


Fig. 11. The Scargle periodogram of the radial velocities of HS 0229+8016 measured from the H α emission line. The periodogram from a set of fake radial velocities is shown in the top panel.

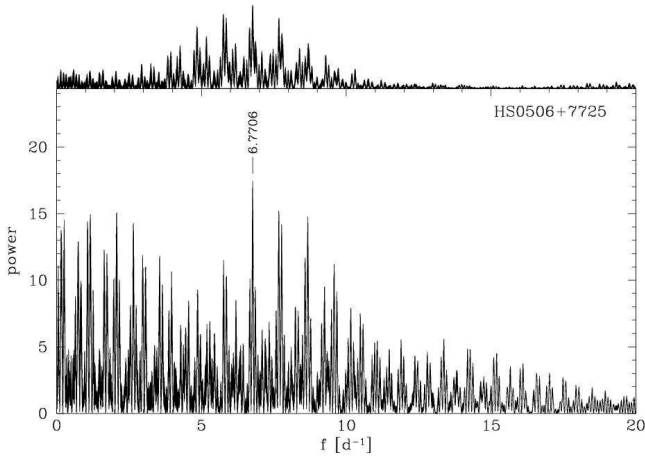


Fig. 12. The Scargle periodogram of the radial velocities of HS 0506+7725 measured from the H α emission line by using the double Gaussian method. The periodogram from a set of fake radial velocities is shown in the top panel.

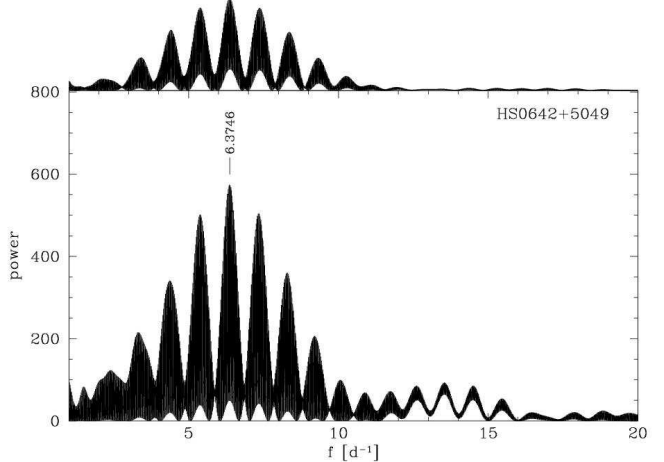


Fig. 13. The Scargle periodogram of HS 0642+5049 computed from the three longest nights of differential photometry obtained at the Calar Alto (2004 October 25) and the IAC80 (2004 December 8 & 9). The periodogram from a fake data set assuming a period of 225.90 min is shown in the top panel

riod or its one-day alias. While our photometric data is not sufficient to improve the period determination of HS 0229+0559, it suggests that the orbital period of HS 0229+0559 can be refined by a sequence of sufficiently long photometric time-series.

4.3. HS 0506+7725

Our initial analysis of the HS 0506+7725 H α radial velocity variation was carried again applying a single-Gaussian convolution on the continuum-normalised line profiles. However, the Scargle periodogram computed from the measured radial velocity variations turned out to be dom-

inated by a variety of signals in the range $\sim 1 - 5 \text{ d}^{-1}$, none of which resulted in a plausible phase-folded radial velocity curve. In a second attempt, we applied the double Gaussian method of Schneider & Young (1980), using a Gaussian FWHM=700 km s $^{-1}$ and a separation of 1500 km s $^{-1}$ which measures the radial velocity variation of the line wings. The Scargle periodogram resulting from these radial velocity measurements includes several peaks in the range 5 – 9 d $^{-1}$ (Fig. 12). The strongest signal is found at $6.7706 \pm 0.0065 \text{ d}^{-1}$, which we identify as the likely orbital period of HS 0506+7725, $P_{\text{orb}} \simeq 212.7 \pm 0.2 \text{ min}$, where the error is determined from a sine fit to the radial velocity data (Table 2). The Scargle peri-

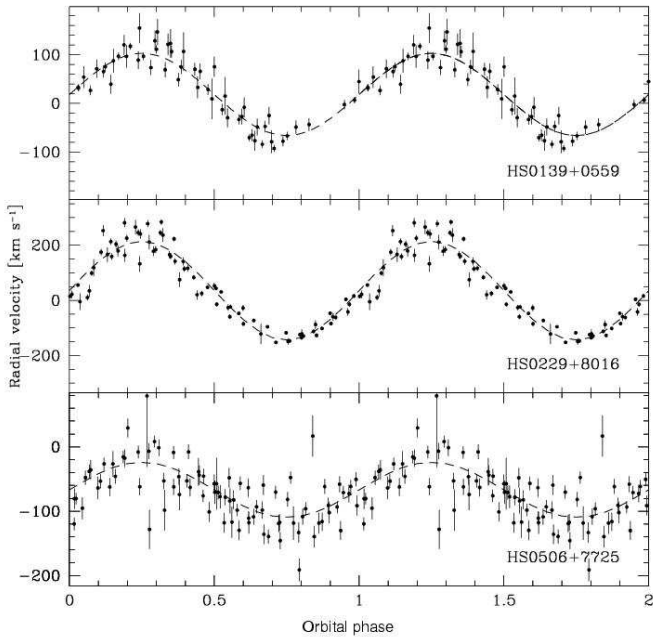


Fig. 14. $H\alpha$ radial velocities of HS 0139+0559 (top panel), HS 0229+8016 (middle panel) and HS 0506+7725 (bottom panel) folded on the period of 243.69 min, 232.550 min and 212.7 min respectively. The dashed lines are the best sine fits to the folded velocities.

odogram computed from a fake data set results in a much cleaner periodogram than that obtained from the observed data, suggesting that the line wings are affected by additional velocity contributions apart from the orbital motion. The $H\alpha$ radial velocities folded over the orbital period (Fig. 14) display a low amplitude of $42.6 \pm 4.4 \text{ km s}^{-1}$ and a relatively large amount of scatter, again suggesting that the orbital motion measured from the line wings is contaminated by another velocity component.

Our time-series analysis of the photometry of HS 0506+7725 did not lead to the detection of any significant signal, either at long (orbital) or at short (putative white dwarf spin) frequencies, making the observed short-term variability (Fig. 8) a nice example of non-coherent CV flickering.

4.4. HS 0642+5049

The 87 available spectra of HS 0642+5049 were subjected to radial velocity studies as outlined above, both using the single-Gaussian and double-Gaussian convolution techniques. None of the resulting Scargle periodograms contained any significant signal. Inspecting trailed spectra assembled from our data, we concluded that HS 0642+5049 does not show any radial velocity variation at our spectral resolution.

Considering the ~ 3.5 h modulation observed in the HS 0642+5049 light curves, we used the three longest and closest spaced photometric data sets obtained at the Calar Alto 2.2 m telescope (2004 October 25) at the IAC80

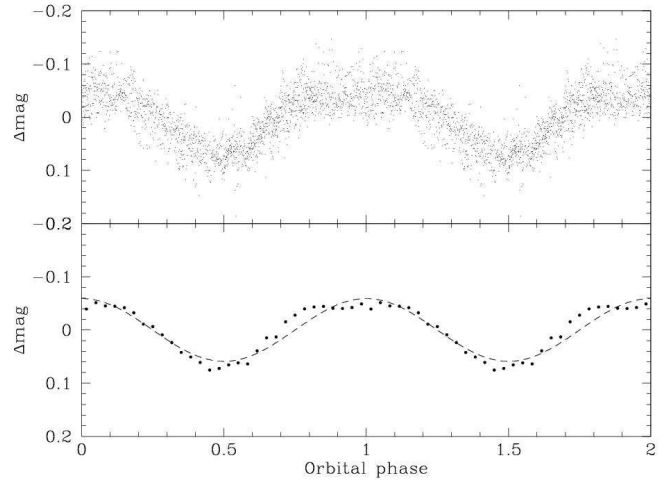


Fig. 15. HS 0642+5049 photometric data from the CAFOS (2004 October 9) and the IAC80 (2004 December 8 & 9) folded on $P_{\text{orb}} = 225.90$ min (top panel). The average light curve, binned into 30 phase is shown in the bottom panel along with a sine fit (dashed line).

(2004 December 8 & 9) to determine the orbital period of the system. The strongest peak detected in the Scargle periodogram computed from these data is found at $6.3746 \pm 0.0065 \text{ d}^{-1}$, surrounded by one-day aliases (Fig. 13). In order to test the significance of the signal, we created a set of fake data from a sine wave with a frequency of 6.3746 evaluated at the exact times of the observations. The alias structures of the periodograms calculated from the fake data and the real data agree well. We conclude that the orbital period of HS 0642+5049 is $P_{\text{orb}} \simeq 225.90 \pm 0.23$ min.

Fig. 15 shows the CAFOS and the IAC80 photometry folded on 225.90 min and averaged into 30 phase bins which reflects the morphology of the individual light curves (Fig. 9).

5. Discussion

5.1. The inventory of the 3–4 h orbital period range

The primary aim of our search for CVs in the HQS is to establish the orbital periods and CV subtypes for a large sample of CVs that were selected in a homogeneous way based on their spectroscopic properties. The properties of this sample will then be compared with the predictions of CV evolution theory. Here, we report the spectroscopic identification and detailed follow-up studies of HS 0139+0559, HS 0229+8016, HS 0506+7725 and HS 0642+5049, which have the orbital periods of 243.69 min, 232.550 min, 212.7 min and 225.90 min, respectively. This follows the trend noticed by Gänsicke et al. (2002b) and more recently by Gänsicke (2004) and Rodríguez-Gil (2005) that the majority of the new CVs identified in the HQS have orbital periods above the period gap and the bulk of them are concentrated in the 3–4 h orbital

Table 2. Sine fits to the H α emission line radial velocities. The methods employed were a convolution with a single Gaussian (SG) or Schneider & Young’s (1980) double-Gaussian prescription (DG).

Object	Method	FWHM/Sep. (km s ⁻¹)	T_0	Period (days)	K (km s ⁻¹)	γ (km s ⁻¹)
HS 0139+0559	SG	600	2452998.985 \pm 0.013	0.16923 \pm 0.00034	84.4 \pm 4.8	18.4 \pm 3.5
HS 0229+8016	SG	600	2452992.457 \pm 0.006	0.161493 \pm 0.000034	179.0 \pm 5.2	35.5 \pm 3.5
HS 0506+7725	DG	700/1500	2452990.679 \pm 0.022	0.14770 \pm 0.00014	42.6 \pm 4.4	-66.7 \pm 3.0

period range. Currently, orbital periods have been determined for 42 systems out of a total of 53 new HQS CVs, and Fig. 16 compares the period distribution of these new HQS CVs with the period distribution of the CVs from the Ritter & Kolb catalogue (2003, V7.4). Even though the follow-up of the new HQS CVs is not yet complete, it is already now clear that our survey *did not* identify the large number of short-period CVs predicted by the population models (e.g. Kolb 1993; Howell et al. 1997), even though our selection method (=detection of Balmer emission lines) is most-suited for the identification of low mass transfer systems, that might be inconspicuous in other ways (variability, X-rays), such as e.g. the short-period dwarf novae HS 1449+6415 (Nogami et al. 2000) and HS 2219+1824 (Rodríguez-Gil et al. 2005a), or the ultra-short period HS 2331+3905, which might be a WZ Sge type dwarf novae with extremely long outburst recurrence times (Araujo-Betancor et al. 2005a). The (somewhat preliminary) conclusion is that if a large number of short-period CVs does indeed exist, they must look different from the well-known examples such as e.g. WZ Sge.

The HQS CV survey has been very prolific in identifying relatively bright long-period CVs, with a distinct preference for the 3–4 h period range (Fig. 16), including the four new CVs presented in this paper. The majority of these new long period CVs are weak or no X-ray emitters, and display little long-term variability – in fact, only five confirmed dwarf novae are among the 28 new systems found above the gap. Gänsicke (2004) and Rodríguez-Gil (2005) pointed out the large frequency of SW Sextantis stars among the new HQS CVs, which represent 25% of all newly identified CVs above the gap, and nearly half of all the new CVs in the 3–4 h period range. For comparison, we show in Fig. 17 the inventory of the 3–4 h orbital period range according to Ritter & Kolb (2003, V7.4). We find that 114 CVs (20% of all CVs with known P_{orb}) inhabit the 3–4 h period range, of which 27 (24%) are confirmed magnetic systems (intermediate polars, polars). 33 (29%) belong to the group of either VY Scl or SW Sex stars, which share similar properties, and are suspected to contain magnetic white dwarfs as well (e.g. Rodríguez-Gil et al. 2001; Hameury & Lasota 2002). While the ratio of definite magnetic CVs in the 3–4 h period range (24%) is already very high compared to the incidence of magnetism in isolated white dwarfs (Liebert et al. 2003), a confirmation of significant mag-

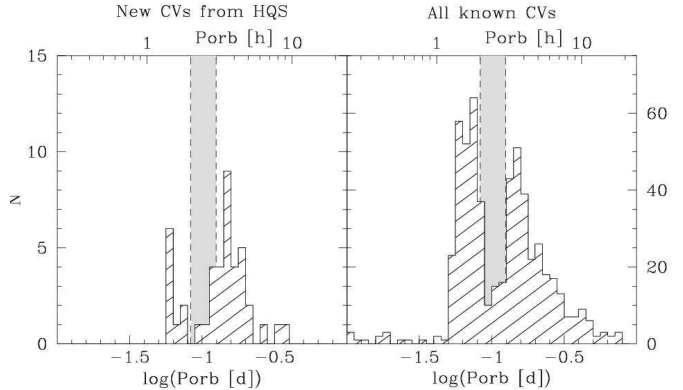


Fig. 16. The period distribution of 42 new CVs discovered in the HQS (left panel) and of all known CVs (right panel, from Ritter & Kolb 2003, V7.4). The 2–3 h period gap is shaded in gray.

netism in the white dwarfs in VY Scl/SW Sex stars would raise the ratio of magnetic/non-magnetic CVs well above 50%, which is in conflict with any of the current models of CV evolution. Whatever the verdict on the magnetic fields in VY Scl/SW Sex stars will be, the large recurrence of this CV subtype suggest that they represent an important phase of CV evolution rather than some unusual combination in their physical properties. For completeness, 32 (28%) novalike variables that do not belong to either the VY Scl or SW Sex class populate the 3–4 h period range². While a number of those systems definitely do not share any of the VY Scl/SW Sex properties, a fair fraction of these systems has been studied only in a very limited way, and hence some of them may join the VY Scl/SW Sex class upon a more detailed scrutiny. Finally, 16 (14%) dwarf novae are known in the 3–4 h period range, the scarcity of systems undergoing thermal disc instabilities just above the period gap is a well-known fact (e.g. Shafter et al. 1986; Shafter 1992).

5.2. The nature of the four new CVs

Based on observational characteristics (summarised in Table 3) we discuss the likely nature of the four new CVs.

² The classification of Ritter & Kolb 2003 is somewhat confusing, as their use of the UX UMa type disagrees with the more common definition of systems characterised by persistent broad Balmer absorption lines.

Table 3. Comparison of the observational characteristics of the four new CVs. The (non)detection of X-ray emission refers to the ROSAT All Sky Survey (Voges et al. 2000). The CV subtypes are abbreviated as UX = UX UMa type novalike variable, ZC = Z Cam type dwarf nova, VY = VY Scl star.

Object	P_{orb} [min]	Radial velocity variation	Photometric variability			X-ray	type
			Orbital	Flickering	Long-term		
HS 0139+0559	243.7	clean, moderate amplitude	none	none	none	no	UX or ZC
HS 0229+8016	232.6	clean, large amplitude	very low amplitude	none	~ 1.3 mag	no	UX or ZC
HS 0506+7725	212.7	scatter, low amplitude	not obvious	large amplitude	~ 3 mag low state	yes	VY
HS 0642+5049	225.9	very low amplitude	moderate amplitude	low amplitude	none	maybe	UX or ZC

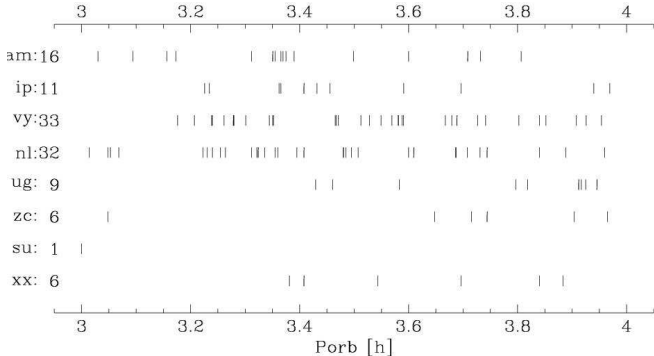


Fig. 17. The period distribution of the individual CV subtypes in the 3–4 h period range. From top to bottom: polars (am), intermediate polars (ip), VY Scl and SW Sex stars (vy), novalike variables and nova remnants that are neither VY Scl nor SW Sex stars (nl), U Gem type dwarf novae (ug), Z Cam type dwarf novae (zc), SU UMa type dwarf novae (su), and systems with undetermined CV subtype (xx).

HS 0506+7725 shows short time scale flickering with quasi-periodic oscillations on time scales of ~ 15 min. The relatively narrow emission lines and the low amplitude of the radial velocity variations suggest a low inclination. The system has been detected in the RASS (Voges et al. 2000) at 0.07 cts s^{-1} (1RXS J051336.1+772836) with a hard spectrum, and has been previously detected as an X-ray source by EINSTEIN (2E 0506.1+7725). The presence of moderately strong He II $\lambda 4686$ emission in the identification spectrum independently confirms the presence of ionising radiation in the system. The detection of a deep low state at $B \simeq 18.3$ on one of the HQS prism plates clearly identifies the system as a VY Scl star. The system does not display *at face value* evidence for being an SW Sex star, but being obviously a low-inclination binary, a spectroscopic study at higher resolution would be useful to test for anomalous radial velocity behaviour in the emission lines.

The other three systems, HS 0139+0559, HS 0229+8016, and HS 0642+5049 are spectroscopically very similar, being characterised by thick-disc absorption line spectra. The fact that we have observed them on various occasions, and found them always at

nearly the same magnitude and with the same spectral properties³ makes it very unlikely that these systems are U Gem-type dwarf novae observed during outburst. While HS 0139+0559 and HS 0229+8016 are not detected in the RASS, a faint X-ray source is found near HS 0642+5049 (1RXS J066618.4+504601, 0.02 cts s^{-1}) which coincides within the $29''$ position error of the RASS detection with the CV. The fact that there are no other nearby objects suggests that HS 0642+5049 is a weak X-ray emitter. None of the systems shows strong flickering activity. One puzzling difference among the three systems is that whereas HS 0139+0559 and HS 0229+8016 show no or only very low-amplitude orbital photometric variability, but exhibit clean quasi-sinusoidal radial velocity variations in their emission lines, HS 0642+5049 does not display any radial velocity variation, but a 0.2 mag photometric modulation. It is very difficult to reconcile this opposite difference in spectroscopic/photometric behaviour in the simple picture of a high-mass transfer CV with a steady-state accretion disc. Based on our data, we identify all three systems either as UX UMa-type novalike variables, or as Z Cam-type dwarf novae observed in periods of standstill. Optical long-term monitoring will be necessary to distinguish between these two possibilities.

6. Conclusions

We have identified HS 0139+0559, HS 0229+8016, HS 0506+7725 and HS 0642+5049 as long-period CVs with the orbital periods of 243.69 ± 0.49 min, 232.550 ± 0.049 min, 212.7 ± 0.2 min and 225.90 ± 0.23 , respectively. HS 0506+7725 is a VY Scl novalike variable characterised by a strong emission-line spectrum. HS 0139+0559, HS 0229+8016 and HS 0642+5049 have thick-disc spectra and are either UX UMa type novalike variables or Z Cam dwarf nova. None of the objects is a strong X-ray source or displays large-amplitude outbursts, which underlines the strength of CV surveys on spectroscopically selected candidates.

³ With one exception: HS 0229+8016 has been observed in August 1992 in a somewhat fainter state, $V \simeq 15.0$, compared to its typical brightness near 14 mag. During that occasion, the Balmer and He I absorption lines were absent/weak, and the strength of the emission lines had markedly increased.

Acknowledgements. AA thanks the Royal Thai Government for a studentship. BTG and PRG were supported by a PPARC Advanced Fellowship and a PDRA grant, respectively. The HQS was supported by the Deutsche Forschungsgemeinschaft through grants Re 353/11 and Re 353/22. Tom Marsh is acknowledged for developing and sharing his reduction and analysis package MOLLY. We thank the referee, Mike Shara, for his comments that lead to an improved presentation of the paper.

References

- Andronov, N., Pinsonneault, M., & Sills, A. 2003, *ApJ*, 582, 358
- Araujo-Betancor, S., Gänsicke, B. T., Hagen, H.-J., et al. 2005a, *A&A*, 430, 629
- Araujo-Betancor, S., Gänsicke, B. T., Hagen, H.-J., Rodríguez-Gil, P., & Engels, D. 2003, *A&A*, 406, 213
- Araujo-Betancor, S., Gänsicke, B. T., Long, K. S., et al. 2005b, *ApJ*, 622, 589
- Barker, J. & Kolb, U. 2003, *MNRAS*, 340, 623
- Bertin, E. & Arnouts, S. 1996, *A&AS*, 117, 393
- de Kool, M. 1992, *A&A*, 261, 188
- Downes, R. A. 1986, *ApJ*, 307, 170
- Downes, R. A., Webbink, R. F., Shara, M. M., et al. 2001, *PASP*, 113, 764
- Gänsicke, B. T. 2004, in *Compact Binaries and Beyond*, ed. G. Tovmassian & E. Sion, Conf. Ser. No. 20 (RMAA), 152–154
- Gänsicke, B. T. 2005, in *The Astrophysics of Cataclysmic Variables and Related Objects*, ed. J.-M. Hameury & J.-P. Lasota (ASP Conf. Ser. 330)
- Gänsicke, B. T., Araujo-Betancor, S., Hagen, H.-J., et al. 2004a, *A&A*, 418, 265
- Gänsicke, B. T., Beuermann, K., & Reinsch, K., eds. 2002a, *The Physics of Cataclysmic Variables and Related Objects* (ASP Conf. Ser. 261)
- Gänsicke, B. T., Fried, R. E., Hagen, H.-J., et al. 2000, *A&A*, 356, L79
- Gänsicke, B. T., Hagen, H. J., & Engels, D. 2002b, in *The Physics of Cataclysmic Variables and Related Objects*, ed. B. T. Gänsicke, K. Beuermann, & K. Reinsch (ASP Conf. Ser. 261), 190–199
- Gänsicke, B. T., Hagen, H.-J., Kube, J., et al. 2002c, in *The Physics of Cataclysmic Variables and Related Objects*, ed. B. T. Gänsicke, K. Beuermann, & K. Reinsch (ASP Conf. Ser. 261), 623–624
- Gänsicke, B. T., Jordan, S., Beuermann, K., et al. 2004b, *ApJ Lett.*, 613, L141
- Hagen, H. J., Groote, D., Engels, D., & Reimers, D. 1995, *A&AS*, 111, 195
- Hameury, J. M. & Lasota, J. P. 2002, *A&A*, 394, 231
- Hameury, J.-M. & Lasota, J.-P., eds. 2005, *The Astrophysics of Cataclysmic Variables and Related Objects* (ASP Conf. Ser. 330)
- Heber, U., Jordan, S., & Weidemann, V. 1991, in *NATO ASIC Proc. 336: White Dwarfs*, 109
- Horne, K. 1986, *PASP*, 98, 609
- Howell, S. B., Rappaport, S., & Politano, M. 1997, *MNRAS*, 287, 929
- King, A. R. 1988, *QJRAS*, 29, 1
- Kolb, U. 1993, *A&A*, 271, 149
- Liebert, J., Bergeron, P., & Holberg, J. B. 2003, *AJ*, 125, 348
- Mennickent, R. E., Tovmassian, G., Zharikov, S. V., et al. 2002, *A&A*, 383, 933
- Nogami, D., Engels, D., Gänsicke, B. T., et al. 2000, *A&A*, 364, 701
- Politano, M. 1996, *ApJ*, 465, 338
- Ringwald, F. A. 1996, in *Cataclysmic Variables and Related Objects*, ed. A. Evans & J. H. Wood, IAU Coll. No. 158 (Dordrecht: Kluwer), 89–92
- Ritter, H. & Burkert, A. 1986, *A&A*, 158, 161
- Ritter, H. & Kolb, U. 2003, *A&A*, 404, 301
- Rodríguez-Gil, P. 2005, in *The Astrophysics of Cataclysmic Variables and Related Objects*, ed. J.-M. Hameury & J.-P. Lasota (ASP Conf. Ser. 330), 335–336
- Rodríguez-Gil, P., Casares, J., Martínez-Pais, I. G., Hakala, P., & Steeghs, D. 2001, *ApJ Lett.*, 548, L49
- Rodríguez-Gil, P., Gänsicke, B. T., Araujo-Betancor, S., & Casares, J. 2004a, *MNRAS*, 349, 367
- Rodríguez-Gil, P., Gänsicke, B. T., Barwig, H., Hagen, H.-J., & Engels, D. 2004b, *A&A*, 424, 647
- Rodríguez-Gil, P., Gänsicke, B. T., Hagen, H.-J., et al. 2005a, *A&A*, 431, 269
- . 2005b, *A&A*, in press (astro-ph/0506055)
- Scargle, J. D. 1982, *ApJ*, 263, 835
- Schenker, K. & King, A. R. 2002, in *The Physics of Cataclysmic Variables and Related Objects*, ed. B. T. Gänsicke, K. Beuermann, & K. Reinsch (ASP Conf. Ser. 261), 242–251
- Schneider, D. P. & Young, P. 1980, *ApJ*, 238, 946
- Shafter, A. W. 1992, *ApJ*, 394, 268
- Shafter, A. W., Wheeler, J. C., & Cannizzo, J. K. 1986, *ApJ*, 305, 261
- Szkody, P., Gänsicke, B. T., Fried, R. E., Heber, U., & Erb, D. K. 2001, *PASP*, 113, 1215
- Szkody, P., Henden, A., Fraser, O. J., et al. 2005, *AJ*, 129, 2386
- Taam, R. E., Sandquist, E. L., & Dubus, G. 2003, *ApJ*, 592, 1124
- Thorstensen, J. R. & Fenton, W. H. 2002, *PASP*, 114, 74
- Voges, W., Aschenbach, B., Boller, T., et al. 2000, *IAU Circ.*, 7432